

# 1

---

## The mathematical modelling of fluidized suspensions

### 1.1 Introduction

At the high concentrations of interest in this book interactions between particles play a major role. These are of two kinds: interactions via motions induced in the interstitial fluid and interactions by direct contact between solid particles. The former dominate when the interstitial fluid is a liquid and the particle concentration is not too large, while the latter dominate when the fluid is a gas, though they may also be important with a liquid medium if the particles are present at very high concentration.

As a result of fluid–particle and particle–particle interactions the behaviour of these systems is very complicated. The distribution of the particles in space is usually far from uniform; the coexistence of regions of strongly contrasting concentration is apparently an intrinsic feature of fluid–particle systems in motion. For many years it was therefore assumed that the properties of these systems could be predicted only by the use of empirical correlations. Many of these were developed and they have since formed the basis for most engineering design, as reflected in the earlier textbooks on the subject; see, for example, Othmer (1956), Leva (1959), and Zenz & Othmer (1960).

Interest in the mechanisms responsible for the observed heterogeneities, and how simple pictures of their associated flow fields might be integrated into design calculations, was sparked by the monograph of Davidson & Harrison (1963) and it dominated the literature of the following decade (Kunii & Levenspiel, 1969). The same period also marked the beginnings of interest in a more fundamental approach, based on equations of motion for the interacting fluid and particles. This was regarded primarily as a means of gaining better understanding of the mechanisms responsible for the complexities of the observed behaviour, rather than as a basis for practical design calculations, and

2      *1. The mathematical modelling of fluidized suspensions*

indeed there was considerable progress of this sort. However, the 1980s saw the dawning of a realization that it might eventually be possible to base quantitative design calculations on differential equations of continuity and momentum balance. Indeed, rapid improvements in the speed and memory capacity of digital computers, coupled with better methods for addressing the difficulties attending numerical solution of the equations of motion, tempted a few pioneers to attempt to predict bubble formation in dense fluidized beds by direct integration of these equations (Pritchett et al., 1978; Gidaspow & Ettehadieh, 1983; Gidaspow et al., 1986).

Though empirical correlations remain, quite properly, a central feature of practical design methods, there is now a rapidly increasing interest in the use of methods that can loosely be described as “computational fluid dynamics”, or CFD. These make it possible to answer many questions that cannot be addressed by using conventional correlations. For example, correlations may be available that are quite successful in predicting the performance of a riser reactor with certain standard arrangements for introducing particles and gas at its foot, but they can say nothing useful about the effect of a proposed change in the detailed geometry of these arrangements, such as replacement of a single entry point for the particles by two or more entry points, or a change in the angle at which a standpipe meets the bottom of the riser. In the case of a dense fluidized bed one might be interested in the effects of proposed internal baffling of specified geometry, in exploring the most effective disposition of immersed heat transfer tubes, or in comparing different designs for the gas distributor. Questions of this sort could, in principle, be addressed if efficient computational codes were available to solve the equations describing the dynamics of the system.

These equations can be formulated at different levels of detail. At the most fundamental level the motion of the whole system is determined by the Newtonian equations of motion for the translation and rotation of each particle and the Navier–Stokes and continuity equations, to be satisfied at every point of the interstitial fluid. These are linked by the no-slip condition between the solid and the fluid on each particle boundary, and the fluid must also satisfy no-slip conditions everywhere on the walls bounding the entire system of interest. Calculations at this level of detail have been performed successfully, but only for quite small numbers of particles. It is not presently conceivable that they could be extended to systems containing the very large number of particles present in commercial units such as fluidized beds.

A second description, at a less detailed level, can be obtained by replacing the fluid velocity at each point by its average, taken over a spatial domain large enough to contain many particles but still small compared to the whole region occupied by the flowing mixture. The force exerted by the fluid on each particle

is then related to the particle's velocity relative to this *locally averaged* fluid velocity, and to the local concentration of the particle assembly, using one of a number of empirical correlations. The Newtonian equations of motion are then solved for each particle separately, taking into account direct collisions between particles when this is appropriate. This procedure, sometimes referred to as "discrete particle modelling", is much less demanding computationally than a complete solution at the first level of detail. Results from this approach have begun to appear in the literature in the past few years (see, for example, Tsuji et al. (1993) and Hoomans et al. (1996)), and their number can be expected to increase.

At a third level of detail both the fluid velocity and the particle velocity are averaged over the local spatial domains introduced above. There are then two local-averaged velocity fields,  $\mathbf{u}$  and  $\mathbf{v}$ , for the fluid and the particles respectively. Each of these is defined at all points of space, so that the resulting equations *look like* the equations of motion one would write for two imaginary fluids, capable of interpenetrating so that every point is occupied simultaneously by both fluids. Consequently, a description at this level of detail is often referred to as a "two fluid model". As we shall see in Chapter 2 the formal process of averaging that leads to these equations leaves behind a number of terms whose form is not determined, and to close the equations they must be related to the fields of  $\mathbf{u}$ ,  $\mathbf{v}$ , and particle concentration. This type of model then takes the form of coupled partial differential equations that usually must be solved numerically, subject only to boundary conditions at the boundaries of the system as a whole. This might be expected to be less demanding computationally than the solution of models at the first and second levels of detail and, as we shall see, there are certain important problems for which approximate, or even exact, analytical solutions can be found. Compared with discrete particle models these two-fluid models suffer from the disadvantage that closures must be formulated for certain important terms left undetermined in the averaged momentum equation for the particle phase. However, it is by no means clear that the physical effects corresponding to these terms are represented properly even by the discrete particle models, since these replace the fluid flow field by its locally averaged form.

This book will deal primarily with the third level of description, that is, the so-called two-fluid models, and what light they have been able to throw on a number of important questions concerning the motion of fluidized particles. This focus is in no way intended to reflect adversely on the enormous and continuing importance of more empirically based approaches, nor on the promise of more detailed models at the first or second levels described above. The former have already been covered well in a number of texts, whereas the latter are still at an early stage of development where it would not yet be appropriate to

4      *1. The mathematical modelling of fluidized suspensions*

summarize them in book form. The specific problems discussed in Chapters 3 to 7, while having intrinsic importance and serving to illustrate the sort of results obtainable using equations of the two-fluid type, also frankly reflect the author's own interests over the past three and a half decades.

It should be emphasized that the point of departure for our averaged equations of motion is the equations at the first level of detail, referred to above, which are well established. The averaging process is then entirely formal and it leaves behind terms that, though not expressed in terms of the average variables themselves, are nonetheless explicitly related to details of the motion at the "microscopic" scale of the individual particles. We resort to empirical closures for these terms only because we do not know, at present, how to evaluate them exactly, except in the simplest cases. This should be contrasted to an alternative approach that, from the outset, "models" the fluid-particle system as a pair of interpenetrating continuous fluids, then formulates their equations of motion using intuitive ideas, constrained by general principles of continuum mechanics. Though both approaches may lead to similar equations there is a clear distinction between their philosophies.

### **1.2 A Simple Application of Equations of the Two-Fluid Type**

Obviously, the equations of motion for a fluid-particle mixture, in local-averaged form, are more complicated than the equations of motion of a single-phase fluid. To begin with, they are larger in number; there are two scalar equations of continuity and two vector equations of momentum balance, with the latter coupled through the forces of interaction between the two phases. Since, even for a single-phase fluid, exact solutions are available only in quite simple situations one might naturally conclude that the scope for making useful deductions from the two-fluid equations is very limited. However, paradoxically, this is not entirely the case. There are situations in which simplifying assumptions, so radical that they would lose the features of physical interest for single-phase flow, still succeed in accounting for important aspects of the behaviour of the two-phase system. We shall now illustrate this by a simple, but practically important example.

Consider fully developed flow in a vertical pipe of circular cross section. For a single-phase incompressible fluid there is then the exact Poiseuille solution that relates the gravity force, the pressure gradient, and the velocity profile. If the fluid is permitted to slip freely in contact with the pipe wall there is a simpler, one-dimensional solution. The velocity is then the same at all points of the cross section, and it is found that the pressure gradient does not depend on the flow rate but is always equal to the hydrostatic gradient induced by gravity.

1.2 A simple application of equations of the two-fluid type 5

However, this solution is of little value since the result of most practical interest, namely the relation between flow rate and pressure gradient, is lost because of the simplification.

For a fluid–particle suspension, in contrast, a comparably radical simplification by no means destroys the usefulness of the solution. A complicated and largely realistic pattern of behaviour can still be predicted, as we shall now demonstrate by means of an example that is both simple and of some practical importance. We shall focus attention on a gas–particle mixture moving up a vertical pipe. Then, permitting free slip of both phases at the pipe wall, we shall seek a solution in which the local average velocity of each phase and the concentration of the particles are all independent of position and time. This means that the flow is steady and fully developed, and both the particle concentration and the velocities of gas and particles are independent of radial position. Then, if  $\phi$  denotes the fraction of the total volume occupied by the particles, and if  $\bar{V}_f$  and  $\bar{V}_s$  denote the volume flow rates of fluid and solid material per unit cross-sectional area, the local average axial velocities of fluid and particles,  $u$  and  $v$ , are given by

$$u = \frac{\bar{V}_f}{1 - \phi}, \quad v = \frac{\bar{V}_s}{\phi}. \quad (1.1)$$

For small enough particles the drag force  $f$ , per unit total volume, exerted by the fluid on the particles would be expected to be proportional to  $u - v$ , with a factor of proportionality  $\beta$  that is an increasing function of  $\phi$ :

$$f = \beta(\phi) \left[ \frac{\bar{V}_f}{1 - \phi} - \frac{\bar{V}_s}{\phi} \right]. \quad (1.2)$$

We shall assume that  $\beta$  is given by a well-known empirical expression due to Richardson & Zaki (1954), namely

$$\beta(\phi) = \frac{\rho_s \phi g}{v_t (1 - \phi)^n}, \quad (1.3)$$

where  $\rho_s$  is the density of the solid material,  $v_t$  is the terminal velocity of fall of an isolated particle in an infinite body of the fluid, and  $n$  is a number whose value depends on the Reynolds number for a particle moving through the fluid with speed  $v_t$ .

As attention is limited to fully developed flow inertial terms vanish and the momentum equation for each phase reduces to a force balance. Since the suspending fluid is a gas, buoyancy forces can also be neglected and, making use of (1.2) and (1.3), a force balance on the particles in unit volume of the

6 1. The mathematical modelling of fluidized suspensions

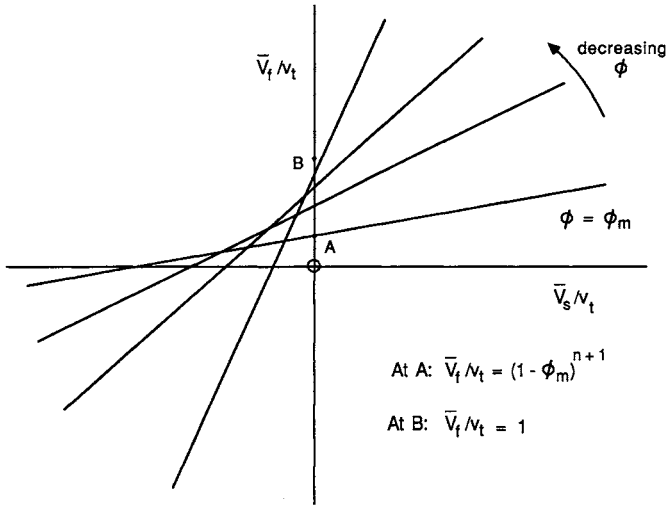


**Figure 1.1.** Contours of constant  $\phi$  (or pressure gradient) in the plane of  $\bar{V}_s/v_t$  and  $\bar{V}_f/v_t$ . (After Jackson, 1993.)

suspension gives

$$\frac{\bar{V}_f/v_t}{1 - \phi} - \frac{\bar{V}_s/v_t}{\phi} = (1 - \phi)^n. \tag{1.4}$$

A corresponding force balance on the gas shows that its pressure gradient must support the weight of the suspended particles, so

$$\frac{dp}{dz} = -\rho_s \phi g, \tag{1.5}$$

where  $z$  is a coordinate measured vertically upward. This indicates that the pressure gradient or  $\phi$  may be invoked interchangeably, since they are proportional to each other.

One way of presenting these relations graphically is as contours of constant  $dp/dz$  (or equivalently  $\phi$ ) in the  $(\bar{V}_s, \bar{V}_f)$ -plane. From (1.4) we see that these are a set of straight lines of slopes  $(1 - \phi)/\phi$ , as shown in Figure 1.1. The line for  $\phi = 0$  coincides with the ordinate axis, while the line of smallest slope corresponds to  $\phi = \phi_m$ , the volume fraction for random close packing. The contours extend into the first, second, and third quadrants, where they represent cocurrent upflow, countercurrent flow, and cocurrent downflow, respectively. Points in the fourth quadrant are, of course, physically impossible since they would represent upward flow of particles with a downward flow of gas. In the second quadrant the set of contours has an envelope, and all points enclosed between this envelope, the positive  $\bar{V}_f$  axis, and the negative  $\bar{V}_s$  axis represent possible

1.2 A simple application of equations of the two-fluid type

7

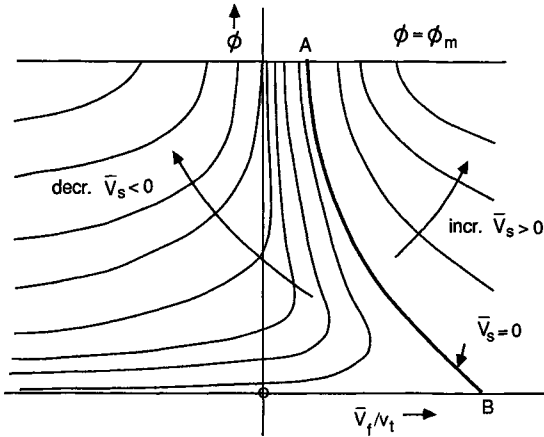


**Figure 1.2.** Zenz diagram (curves of constant  $\bar{V}_s$  in the plane of  $\bar{V}_f/v_t$  and  $\phi$ ) corresponding to Figure 1.1. (After Jackson, 1993.)

conditions for countercurrent flow. This region is of bounded extent because countercurrent flow is not possible for arbitrarily large values of either the gas flow or the particle phase flow. Points on the envelope correspond to conditions usually referred to as “flooding”.

A second method of graphical presentation is the so-called Zenz diagram, which shows a set of curves relating the pressure gradient (or equivalently  $\phi$ ) to the gas flow rate, for various fixed values of the particle flow rate. It is easy to translate Figure 1.1 into this alternative form and the result is sketched as Figure 1.2, where  $\phi$  is used as the ordinate. The curve labelled AB, which corresponds to  $\bar{V}_s = 0$ , represents situations in which the particles are suspended at rest in the flowing gas – in other words, fluidized beds. The corresponding part of Figure 1.1 is the interval AB of the ordinate axis. The part of Figure 1.2 to the right of AB represents cocurrent upflow, the part between AB and the axis  $\bar{V}_f = 0$  represents countercurrent flow, and the whole region  $\bar{V}_f < 0$  represents cocurrent downflow.

We have already noted that this very simple theoretical model predicts flooding in countercurrent flow. It can also be used to illustrate another striking aspect of suspension flow, namely the importance of interactions between the pipe itself and the devices used to supply the gas and the particles. Let us focus on the characteristics of the gas supply device, assuming that some provision has been made to feed the particles at the constant flow rate represented by  $\bar{V}_s$ . We envisage a system in which gas starting from atmospheric pressure is compressed and introduced at the bottom of the vertical pipe, where it is joined by the particles, while at the top of the pipe the suspension is discharged into a

8 1. The mathematical modelling of fluidized suspensions

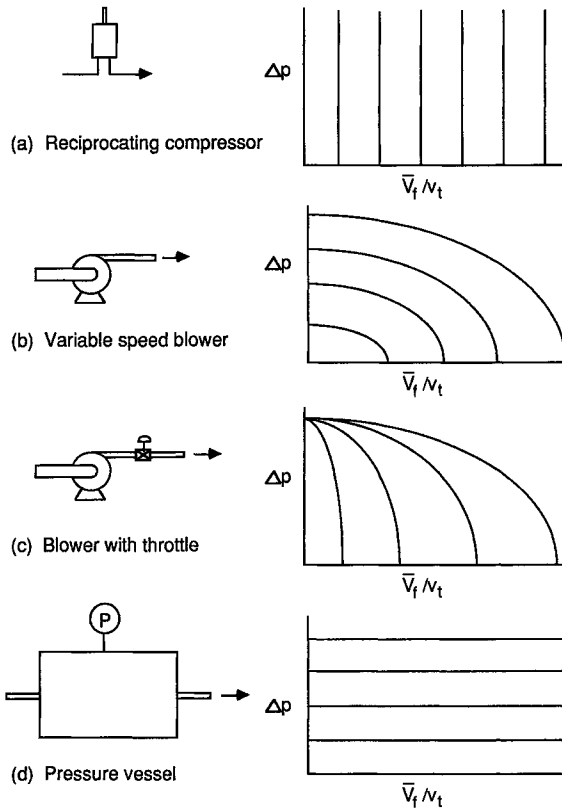


**Figure 1.3.** Characteristics of different types of gas compression device. (After Jackson, 1993.)

second region, also at atmospheric pressure. Then the device used to compress the gas must raise its pressure by an amount that exactly balances the drop in gas pressure along the pipe. Denote the magnitude of each of these pressure changes by  $\Delta p$ .

In general the pressure rise across the gas compression device is related to the flow rate, and a curve showing this relation is called a *characteristic* of the device. Figure 1.3 shows sketches of these characteristics for various devices.

Panel (a) represents an idealized reciprocating compressor, for which the flow rate is almost independent of  $\Delta p$ . Panel (b) is a centrifugal blower whose speed can be adjusted. There is then a separate characteristic curve for each value of the speed, and on each curve  $\Delta p$  decreases as the delivered flow increases, falling to zero at some finite value of the flow. Panel (c) again represents a centrifugal blower, but in this case the speed is constant and a throttle valve

1.2 A simple application of equations of the two-fluid type

9

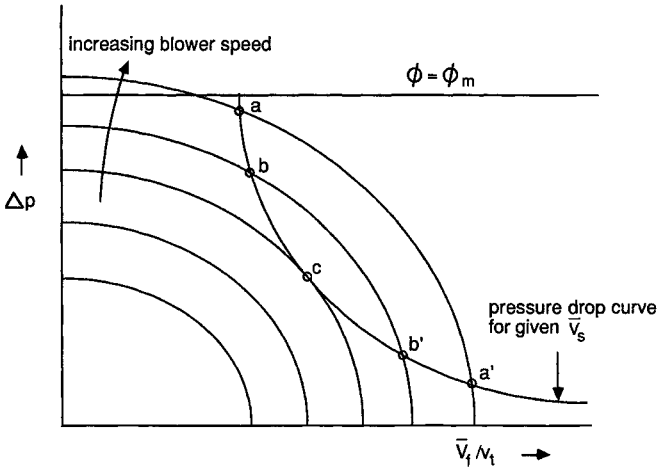


**Figure 1.4.** Determination of operating conditions by superimposing the pressure drop curve for the pipe and the characteristic curves of a variable speed blower. (After Jackson, 1993.)

in the delivery line is used for control. Then there is a separate characteristic curve for each setting of this valve, as indicated. Finally, panel (d) shows a large pressurized buffer vessel as a source of the gas. The pressure to which this is charged then determines  $\Delta p$ , and the characteristics are horizontal lines, one for each value of this pressure.

The operating conditions for the combination of the gas compression device and the pipe are determined by the intersection of the characteristic curve of the compression device with the curve from the Zenz diagram relating  $\Delta p$  to  $\bar{V}_f$  for the pipe. This latter curve is obtained from Figure 1.2 by scaling the curve for the appropriate value of  $\bar{V}_s$  by a multiplier  $\rho_s g L$ , where  $L$  is the total length of the pipe. For compression device characteristics of the types shown in panels (a) and (d) of Figure 1.3 the intersection in question is clearly unique, but this is not so for the blower characteristics of panels (b) and (c). Figure 1.4 superimposes the pressure drop curve for the pipe, for the specified value of  $\bar{V}_s$ , and several blower characteristics from panel (b) of Figure 1.3; we see that the number of intersections is either two or zero, depending on the blower speed. If the blower speed is high there are two, such as the points denoted by  $a$  and  $a'$ , and as the blower speed is progressively decreased these move closer together, as seen from the pair  $bb'$ . Finally a critical value of the blower speed is reached at which the intersection points coincide (point  $c$ ), and for lower speeds there is no intersection, indicating that the particles can no longer ascend the pipe as a suspension in the gas. This represents a condition called “choking”; when the

10 *1. The mathematical modelling of fluidized suspensions*

speed falls below this value there is a discontinuous increase in  $\phi$  to the value  $\phi_m$  and the particles continue to ascend the pipe at the specified flow rate only if they can be forced up as a packed bed by the particles injected below them.

When the blower speed is high enough to avoid choking the question remains as to which of the two intersection points represents the actual operating condition of the system. This raises the issue of stability, which can be addressed either intuitively or more formally. At any point in Figure 1.4 representing an operating state the pressure rise in the gas feed device balances the pressure drop in the pipe. If, as a consequence of a small increase in the gas flow rate, the pressure rise in the compression device should become larger than the pressure drop in the pipe, intuition would suggest that the original operating point was unstable. Conversely, if a small increase in the gas flow rate causes the pressure rise in the compression device to become smaller than the pressure drop in the pipe, one would anticipate stability. A more formal analysis confirms these intuitive ideas (Matsumoto, 1986); so we conclude that points a and b in Figure 1.4 represent unstable conditions of operation, whereas points such as a' and b', lying to the right of point c, represent conditions that are stable and could therefore be observed in practice. The same criterion applied to other gas feed devices indicates that the device of panel (a) in Figure 1.3 gives unique and stable operating points in all cases, whereas the device of panel (d) would always lead to unstable operation. Consequently a feed device whose characteristics approximate sufficiently closely those of panel (a) will exhibit no choking phenomenon as the gas flow is decreased; instead the particle concentration will increase in a continuous way, eventually forming a dense, moving suspension known as a "fast fluidized bed".

Of course, the fact that the operating conditions are determined by an interaction between the pipe and its feed device comes as no surprise; the same is true for the flow of a single-phase fluid. The interesting features of the two-phase flow are the marked qualitative changes, such as flooding and choking, and the influence of the feed device on the whole pattern of behaviour as the flow rates are changed. These have no analogues in the case of single-phase flow.

In single-phase flow the tangential forces exerted on the fluid at the walls of the pipe give rise to the part of the pressure drop that increases with the flow rate. Though these forces have been omitted in the above discussion, they are also present in the suspension flow, and it is not difficult to see how they affect the outcome. For a given value of the particle flow rate we expect that they will make a contribution to the pressure drop in the pipe that increases with increasing gas flow rate. At low flow rates this contribution will be proportional to  $\bar{V}_f$ , and at high flow rates to  $\bar{V}_f^2$ , so the curves of Figure 1.2 are modified as in Figure 1.5, which shows only those corresponding to cocurrent upflow. In